Chapter 5 The Magnetosphere

A Introduction

In the absence of an interplanetary plasma, the earth's dipole field would extend indefinitely in all directions. However, the geomagnetic field produces a semipermeable obstacle to the solar wind and the resulting interaction produces a cavity around which most of the plasma flows. The extent of this obstacle, called the magnetosphere, is related to the solar wind density and velocity and the interplanetary magnetic field (IMF). This cavity is filled by plasma which largely originates in the earth's upper atmosphere.

We may thus describe the magnetosphere (Figures 4.1 and 5.1) as the region of space surrounding the earth in which the geomagnetic field plays a dominant role. Before describing this region we need to do some more basic physics.

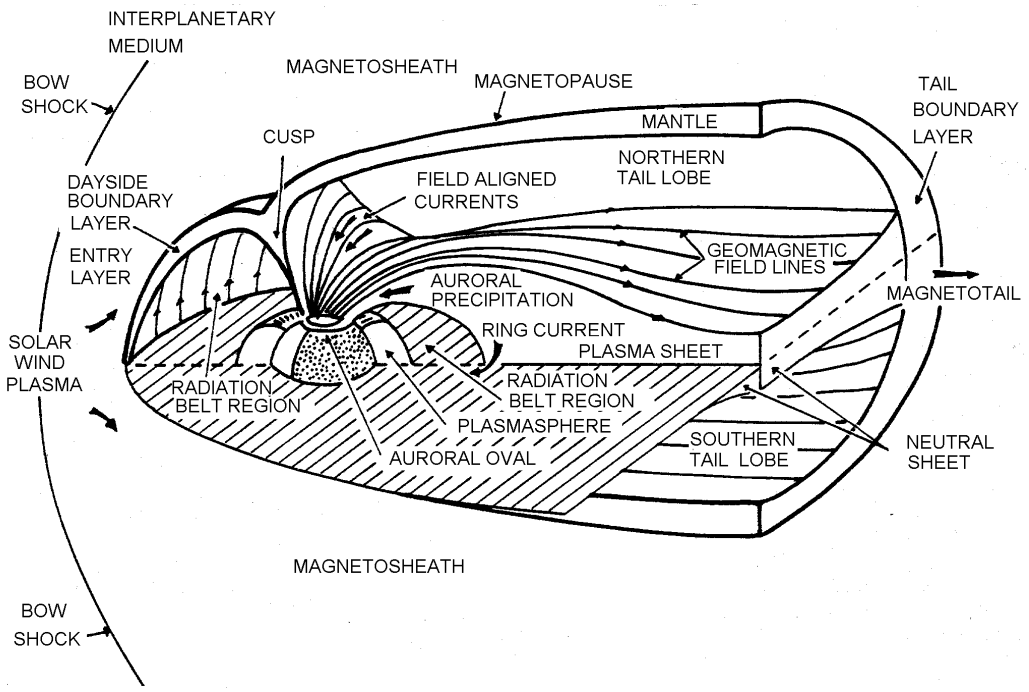

Figure 5.1 The Magnetosphere

B Plasma Physics

1 The Magnetic Moment and Mirroring

Let us begin by defining two quantities which are needed to develop the concept of magnetic mirroring. These are the magnetic flux through a surface, and the magnetic moment. The magnetic moment is one of the most useful concepts in magnetospheric physics, indeed all of plasma physics. It is almost always a conserved quantity, and hence enormously useful in determining the behavior of charged particles.

The magnetic moment of acurrent loop is defined (see figure 5.2) as a vector, $\vec{\mu}$, given by

$$\vec{\mu} = i\vec{A} \qquad \text{(Eqn. 5.1)}$$

Here, i is the circulating current, and **A** is the area vector, defined as positive outward from a closed surface. For a flat surface we use the right hand rule to define the positive direction. In order to make this quantity useful, we need to relate it to two important characteristics of the plasma - the kinetic energy of the charged particles, and the strength of the ambient magnetic field.

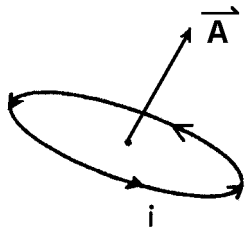

Figure 5.2

Consider now the case where the current i consists of a single circulating particle of charge q, in an external magnetic field, **B**. This circulating charge represents a current:

$$i = \mathrm{q f_c} = q\,\omega_c/2\pi$$

where ω_c is the cyclotron- or gyro- frequency (in radians/second) in an external magnetic field. The magnetic moment of the orbit is:

$$\mu = \mathrm{iA} = (\mathrm{q}\omega_c/2\pi)(\pi\ \mathrm{r_c^2}) \qquad \text{(Eqn. 5.2)}$$

We have from before:

$\omega_c = \mathrm{qB/m}$ and $\mathrm{r_c} = \mathrm{mv_\perp/qB}$

where $\mathrm{v_\perp}$ is the component of the velocity vector perpendicular to $\vec{\mathbf{B}}$.

Plugging these into equation 5.2 gives us:

$$\mu = \left(\frac{\mathrm{q^2B}}{2\,\mathrm{m}}\right)\left(\frac{\mathrm{m^2 v_\perp^{\,2}}}{\mathrm{q^2B^2}}\right) = \frac{\frac{1}{2}\,\mathrm{mv_\perp^2}}{\mathrm{B}}$$

or

$$\mu = \frac{\mathrm{K_\perp}}{\mathrm{B}} \qquad \text{(Eqn 5.3)}$$

Here, $K_\perp$ represents the part of the particles kinetic energy which is associated with the velocity component perpendicular to B. The division of the velocity vector between field-aligned and perpendicular components requires the definition of a new concept - the "pitch angle". Figure 5.3 illustrates the concept.

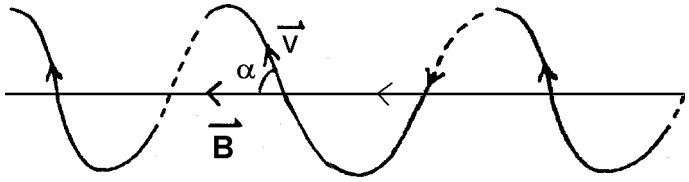

Figure 5.3 - Illustration of pitch angle definition (α). Note that the pitch of a screw is the same concept.

We see from figure 5.3 that:

$$v_\perp = v \sin(\alpha) \qquad \text{(Eqn. 5.4)}$$

and hence the magnetic moment (μ) is:

$$\mu = \frac{\frac{1}{2} m v^2 \sin^2(\alpha)}{B} \qquad \text{(Eqn. 5.5)}$$

Why is this quantity conserved? The answer lies in Faraday's Law (and Lenz's Law; Halliday and Resnick, Fundamentals of Physics, chapter 32 of the third edition)

Recall that the magnetic flux, ϕ , through a given surface is defined (see figure 5.2) as:

$$\phi = \int_S \vec{B} \cdot d\vec{S} \qquad \text{Eqn 5.6}$$

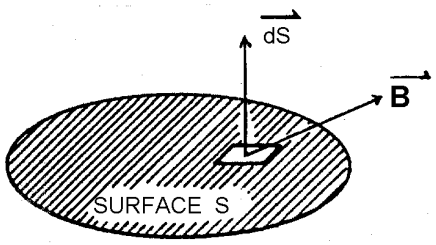

Figure 5.4

This quantity is, in some sense, the "amount" of field which crosses the surface defined by **S.** It's units are Tesla-meter-squared (Tm^2) , or the Weber (W). What is the relationship between this quantity and the magnetic moment? It turns out that they are the same, within a (constant) fudge factor.

$$\phi = B (\pi r_c^2) \qquad \text{(Eqn. 5.6)}$$

(for reasonably constant B)

$$= \pi B \left(\frac{m^2 v_\perp^2}{q^2 B^2} \right) = \frac{2\pi m}{q^2} \left(\frac{m v_\perp^2}{2B} \right) \qquad \text{(Eqn. 5.7)}$$

or

$$\phi = \frac{2\pi m}{q^2} \mu \qquad \text{(Eqn. 5.8)}$$

Faraday's Law says that a voltage, or emf, ε, will be induced around the orbit if Φ changes in time.

$$\mathcal{E} = \frac{-d\,\Phi}{dt} \qquad \text{(Eqn. 5.9)}$$

(Lenz's law then applies this to indicate that attempts to change the magnetic flux through a loop will induce a current in just such a way as to oppose the change in flux.) How does this apply in a plasma? Consider the case where the particle is moving (typically along the magnetic field), and the amplitude of the magnetic field is changing. What happens to the magnetic flux?

A first look at Faraday's law suggests a problem. The emf produced by the changing magnetic flux would result in an acceleration of our charge and hence a change in its kinetic energy. We know, however, that the total kinetic energy of our particle does not change (static magnetic fields can not do work!), which implies that Φ = a constant (through the orbit). How do we resolve this contradiction? Nature resolves this apparent contradiction by forcing the pitch angle to change.

Therefore

$$\mu = \frac{\tfrac{1}{2}mv^2 \sin^2(\alpha)}{B} = \text{a constant} \qquad \text{(Eqn. 5.10)}$$

What is the net effect of this? As the particle penetrates into regions of larger magnetic field (**B**), the pitch angle (α) must increase in order to keep the magnetic moment, μ, constant. Sooner or later α will equal 90° and the longitudinal motion stops. Careful analysis shows that there is a small, non-zero force in a converging magnetic field geometry which produces this effect.

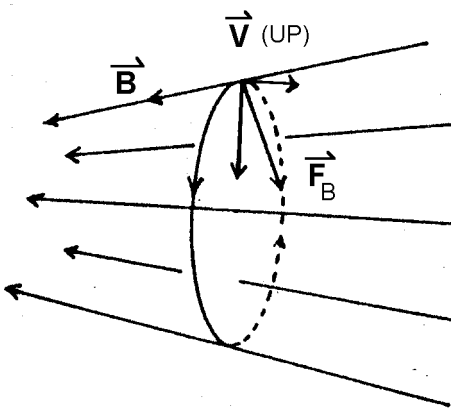

Figure 5.5
The magnetic force, F_B, will have a component in the plane of the orbit and a longitudinal component pointing into the region of lower magnetic field (to the right, here).

If the pitch angle is 90° at the point where the magnetic field is B_M, then

$$\frac{\tfrac{1}{2}mv^2 \sin^2(\alpha)}{B} = \frac{\tfrac{1}{2}mv^2 \sin^2(90°)}{B_M} \Rightarrow \sin^2(\alpha) = B/B_M \qquad \text{(Eqn. 5.11)}$$

where α is the pitch angle at the position where the field is B, and B_M is the value of the field where the pitch angle becomes 90° and the particle is reflected (i.e. mirrors).

Example: the initial pitch angle of a particle at the magnetic equator is 30°, so $\sin^2\alpha = 0.25$, hence the ratio of the magnetic field at the mirror point to that at the equator is 4:1. If the equatorial magnetic field had a value of 100 nT (as at geosynchronous orbit), it would mirror at a latitude where B = 400 nT.

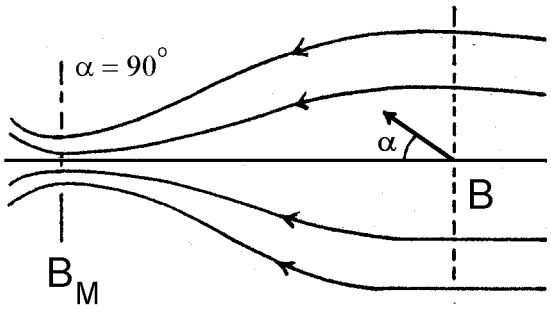

Figure 5.6 - magnetic field lines converge to the left

The concept of the loss cone can now be developed. This idea is important for understanding how particles are lost in the magnetosphere.

If we rewrite the mirror condition, found above, as: $\frac{\sin^2(\alpha)}{B} = \frac{\sin^2(\alpha_M)}{B_M}$

we can see that particles whose pitch angle at a magnetic field strength, B, is less than α will have $\alpha_m < 90°$, and hence will not be reflected and can pass through the mirror region. This is generally the means by which particles escape such magnetic field geometries. Typically, satellite measurements are made at or near the magnetic equator, and this is the minimum B region in the above model. The mirror point, then is at the top of the atmosphere, at high latitude, where the field is much stronger.

Example:

Start at the magnetic equator, at an altitude of one earth radius. Take the magnetic field strength to be 3.75×10^{-6} Tesla, and look for a mirror altitude near the surface of the earth, $B = 4.5\times10^{-5}$ T. Mirroring will occur at or before that point if α meets the condition:

$$\frac{\sin^2(\alpha)}{3.75\times10^{-6}} = \frac{\sin^2(90)}{4.5\times10^{-5}} \text{ or` } \sin^2(\alpha) = \frac{3.75\times10^{-6}}{4.5\times10^{-5}} = 0.083$$

giving $\alpha = 16.8°$. Particles with equatorial pitch angles less than this value will not mirror, and hence will hit the surface of the earth.

We thus see that the charged particle which in general will execute a spiral motion around a given field line will move from the equator into a region of higher magnetic field and that we thus have the likelihood of mirroring occurring, as illustrated in figures 5.6 and 5.7.

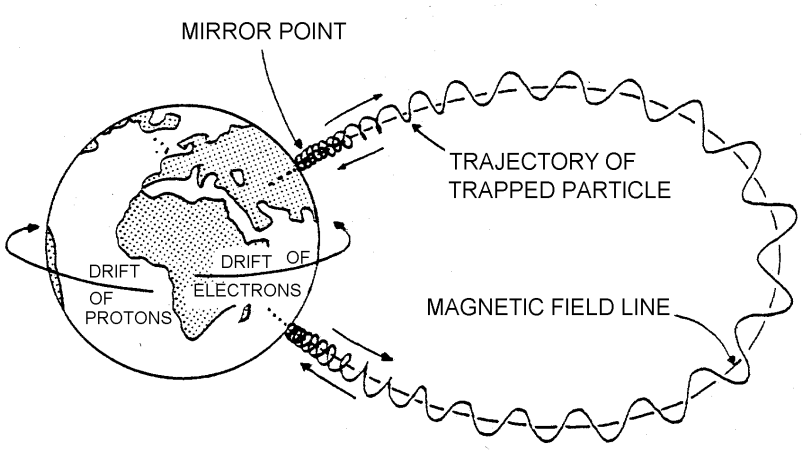

Figure 5.7 Motion of charged particles trapped by the earth's magnetic field. The mirror point is the position where a charged particle stops and changes direction (i.e. a trapped particle bounces between its mirror points). Besides the two-degree motion of spiraling back-and-forth along the field line, the charged particles also have a third degree of motion, a drift around the earth. Notice that electrons drift eastward and protons drift westward, and the resulting charge separation produces a ring current system (After Stern and Ness, 1981).

Consider a particle which has a pitch angle α_0 when it crosses the equatorial plane where the field is B_0. We saw above that the particle will not mirror if the angle α_0 is less than α_c given by:

$$\sin^2(\alpha_c) = B_0 / B_M \qquad \text{(Eqn. 5.12)}$$

where B_M = Mirror field strength

Figure 5.8 Mirror latitudes in a dipole magnetic field

Figure 5.8 presents the relationship between the equatorial pitch angle, α_0, the required ratio of the mirror field B_M to equatorial field B_o and the latitude at which the particle will mirror. If we decrease the equatorial pitch angle α_0, the required magnetic field ratio, B_M/B_o, increases. this means that the particles will mirror at higher latitudes. Since there is a maximum value of B_M which can be reached along any magnetic field line (before hitting the atmosphere), particles with initial pitch angles which are small enough will not be mirrored.

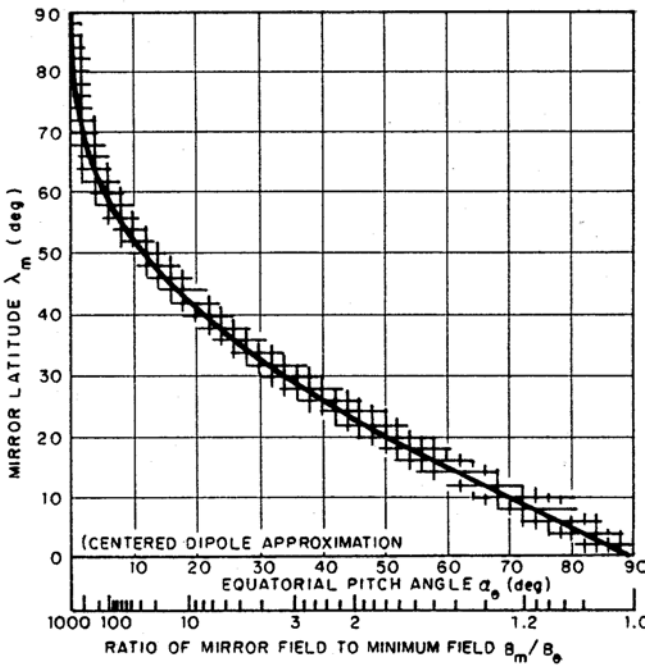

2 Drifts

In addition to the gyration and bounce motions, the entire plane of the particle trajectory will precess in the azimuthal direction around the earth. This component of the motion is essentially a drift motion caused by the fact that the field is not uniform. The dipole magnetic field has both a gradient and curvature at each point. These cause drifts, much as the external electric or gravitational fields were shown to cause drifts.

We can show that the net force on a particle of magnetic moment μ in a non-homogeneous magnetic field is given by:

$$\vec{F} = -\mu \nabla \left|\vec{B}\right| \qquad \text{(Eqn. 5.13)}$$

Since in general the drift velocity is given by:

$$\vec{v}_D = \frac{1}{q}\frac{\vec{F}\times\vec{B}}{B^2} \qquad \text{(Eqn. 5.14)}$$

we get for the gradient drift (or so-called grad-B drift):

$$\vec{V}_D = \frac{-\mu}{q}\frac{\nabla\left|\vec{B}\right| \times \vec{B}}{B^2} = \frac{\mu}{q}\frac{\vec{B} \times \nabla\left|\vec{B}\right|}{B^2} \qquad \text{(Eqn. 5.15)}$$

This can also be expressed in terms of the transverse (or perpendicular) kinetic energy, since we had from the definition of the magnetic moment:

$$\mu = \frac{K_{\perp}}{B} = \frac{\frac{1}{2} m v_{\perp}^2}{B}$$

the drift velocity can therefore be expressed:

$$\vec{v}_D = \frac{K_{\perp}}{qB}\frac{\vec{B}\times\nabla B}{B^2} \qquad \text{(Eqn. 5.16)}$$

This drift is associated with variations in the strength of the magnetic field, in directions perpendicular to B. For a dipole field, this is primarily the variation in magnitude with radius. There is also a term associated with the shape of the field, termed the curvature drift. It can be thought of as a result of the centrifugal force exerted on a particle moving along a curved magnetic field line. The magnitude of this force is:

$$F_c = \frac{mv_{||}^2}{R} \qquad \text{Eqn. 5.17}$$

Here, $v_{||}$ is the velocity component of the particle along the magnetic field line (v cos α), and R is the radius of curvature of the field line along which the guiding center is moving. This results in the curvature drift given by:

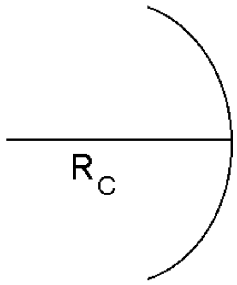

Figure 5.9 Magnetic field lines curve with radius R

$$\vec{\mathbf{v}}_c = \frac{mv_{||}^2}{qR_c^2}\frac{\vec{\mathbf{R}}_c \times \vec{\mathbf{B}}}{B^2} \qquad \text{(Eqn. 5.18)}$$

The curvature and gradient of a magnetic field are intimately related, due to the need to satisfy Maxwell's equations. This is particularly so in a dipole field. We can combine the terms for the gradient and curvature drift to give:

$$\vec{V}_D + \vec{V}_c = \frac{m}{q}\frac{\vec{R}_c \times \vec{B}}{R_c^2 B^2}\left(v_{||}^2 + \tfrac{1}{2}v_{\perp}^2\right) \qquad \text{(Eqn. 5.19)}$$

$$= \frac{m}{q}\frac{\vec{\mathbf{B}} \times \nabla B}{B^3}\left(v_{||}^2 + \tfrac{1}{2}v_{\perp}^2\right)$$

where we have made use of the identity:

$$\frac{\nabla B}{B} = -\frac{\vec{\mathbf{R}}_c}{R_c^2}$$

The precession of the "bounce plane" is due to the drifts given by Eqn. 5.19 above with the directions of precession for positive and negative charges as shown in Figure 5.7. Positive charges drift west, negative charges drift east. Both signs contribute to a current which is westward.

The totality of these gyrating, bouncing and precessing protons (and other ions) and electrons constitute the radiation belts, often referred to as the Van Allen Belts, after their discoverer (and the students who did the work....)

3 Characteristic Time Scales

The corresponding time scales for a 1 MeV particle at an altitude of 2000 km are:

	Electrons	Protons
Gyration Period	7×10^{-6} sec	4×10^{-3} sec
Bounce Period	0.1 sec	2.2 sec
Drift Period	53 minutes	32 minutes

(Differences here are due to the fact that at these energies, the electrons are highly relativistic, and all the relativistic terms we've ignored come into play.)

The substantial difference in characteristic time scales for each of the three characteristic motions makes it possible to consider the motions as decoupled from each other. This enables a great simplification of our studies.

Example:

As we saw in Chapter 1 the gyration period is independent of the energy of the particle and is a function of the mass/charge ratio and the magnetic field only. In general

$T_c = 2\pi \frac{m}{qB}$ which gives for

Protons: $T_c\,(\text{sec}) = \frac{6.51\times 10^{-8}}{B(\text{Tesla})}$ or $T_c\,(\text{sec}) = \frac{6.51\times 10}{B(\text{nT})}$

Electrons: $T_c\,(\text{sec}) = \frac{3.5\times 10^{-11}}{B(\text{Tesla})}$ or $T_c\,(\text{sec}) = \frac{3.55\times 10^{-2}}{B(\text{nT})}$

Taking B = 10^4 nT as a typical value in the radiation belts we see that proton gyroperiods are typically in the millisecond range and electrons in the microseconds.

4 McIlwain L and Invariant Latitude

As we move into the magnetosphere, we need to define a particularly useful coordinate system. This system makes use of the fact that particles move along magnetic field lines, as developed above. Carl McIlwain developed the "L" parameter to provide a handy label for the magnetic field lines, and the McIlwain L-value is used throughout space physics. The L-value for a given magnetic field line is determined by (equal to) the distance from the center of the earth to the point at which it crosses the magnetic equator. The complementary parameter which is then needed to locate a region of interest is the magnetic latitude, λ_m. The ordered pair, (L, λ_m), along with local time or longitude, then uniquely determines a location in space. The units of "L" are earth radii, magnetic latitude is typically given in degrees, and local time is generally preferred for the third coordinate. Thus the line which crosses the equator at r = 3 earth radii is labeled L = 3.

It can be shown that the radial distance, r, and latitude, or more properly, magnetic latitude (λ_m) are related according to the form:

$$\frac{r}{R_E} = L \cos^2 \lambda_m \qquad \text{(Eqn. 5.20)}$$

Again, we distinguish between the latitude, λ, and the magnetic latitude, λ_m.

The above expression is useful for all values of $\lambda_m < \Lambda_c$. Λ_c is the latitude at which a given line reenters the earth. This maximum latitude is given by

$$\cos \Lambda_c = \frac{1}{\sqrt{L}} \qquad \text{(Eqn. 5.21)}$$

Λ_c, or simply Λ is termed the invariant latitude, since, like L, it does not vary along the field line. In general, geophysicists specializing in the ionosphere use Λ, magnetospheric specialists use L.

The magnitude of the magnetic field is now given by:

$$B = \frac{B_{os}}{L^3} \frac{\sqrt{4 - 3 \cos^2 \lambda_m}}{\cos^6 \lambda_m} \qquad \text{(Eqn. 5.22)}$$

where:

B_{os} = Equatorial Field at the surface (equator)

Example:

How does the magnitude of the magnetic field vary with latitude (λ_m) along a magnetic field line, that is along a line of constant "L", or Λ. Beginning with equation 5.21, we use the values:

$L = 5.6$, $\Lambda = 65°$, and assume $B_{os} = 30{,}000$ nT

we obtain the values:

$$B\left(L = 5.6,\ \lambda_m = 0°\right) = 1.00\left(B_{os}/176\right) = 170 \text{ nT}$$
$$B\left(\lambda_m = 30°\right) = 3.14\left(B_{os}/176\right) = 534 \text{ nT}$$
$$B\left(\lambda_m = 45°\right) = 12.65\left(B_{os}/176\right) = 2{,}150 \text{ nT}$$
$$B\left(\lambda_m = 60°\right) = 115.4\left(B_{os}/176\right) = 19{,}618 \text{ nT}$$

Increase B as function of λ_m for the same L value, not the same r.

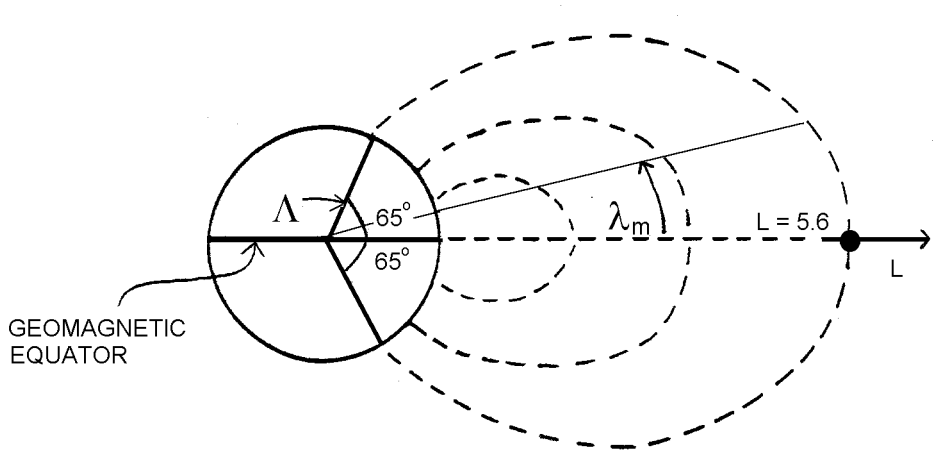

Figure 5.10 Magnetic field lines reach the surface of the earth at a latitude termed the Invariant Latitude.

C Magnetosphere structure

Returning now to the magnetosphere, we find the main features of the magnetosphere are (see Fig 5.1)

(1) Bow Shock: Where the initial deceleration and deflection of solar wind particles occurs

(2) Magnetopause: The outer boundary of the magnetosphere which divides magnetosphere and solar wind plasma.

(3) Neutral Sheet: Extends behind the earth in the antisolar direction. Divides the geomagnetic tail into lobes with B lines pointing toward and away from the earth.

(4) Plasma Sheet: A region of moderate particle density surrounding the neutral sheet. The plasma sheet is magnetically connected to the auroral ovals.

(5) Trapped Radiation Belts: A region in which high energy electrons & protons gyrate around closed magnetic field lines between mirror points.

(6) Plasmasphere: A region of relatively cold plasma (energies < 1 eV) which corotates with the earth due to frictional coupling.

(7) Cusps: Regions which divide the magnetic field lines which close on the earth surface (sunlit side) from those which are stretched out into the tail.

Next let us consider some of these in a little more detail, starting with the bow shock which is the first thing the solar wind runs into as it approaches the earth.

D Bow Shock:

The observed shock wave in the solar wind is the result of a collective plasma interaction, usually referred to as a collisionless shock. It has some similarities to the aerodynamic shock formed around blunt objects but the mechanism by which the individual particles interact is not the same. In the aerodynamic case it is the actual collision of gas particles and the shock thickness is determined by the mean free path between collisions.

In the solar wind the mean free path is on the order of 10^8 km which is much larger than the radius of the earth. In fact the bow shock is not a collisional aerodynamic shock but is due to electromagnetic interaction between the magnetized solar wind (frozen-in field lines) and the magnetosphere. The aerodynamic formulas work reasonably well because the frozen-in field lines limit the particle motion of the solar wind plasma perpendicular to the field. This constraint makes the otherwise collisionless solar wind act like a collision dominated fluid (at least as far as motion perpendicular to the field is concerned).

We can estimate the thickness of the shock to be on the order of the gyration radius in the solar wind

$$r_c = \frac{mv}{qB} = \frac{\left(1.67\times10^{-27}\right)\left(5\times10^{4}\right)}{\left(1.6\times10^{-19}\right)\left(10^{-8}\right)} \cong 50 \text{ km}$$

Where we have assumed protons of mass $1.67\text{x}10^{-27}$ kg with a transverse speed of $5\text{x}10^{4}$ m/s which corresponds to a temperature in the solar wind of 10^5 °K. We have also assumed a local magnetic field of about 10 nT which agrees with measured values.

We thus find that the bow shock has a thickness on the order of 50-100 km.

It can also be shown that the ratios of particle velocity and particle density are approximately those predicted by theory, namely

$$V_{postshock} = \frac{1}{4}V_{preshock} \quad \text{and} \quad \rho_{preshock} = \frac{1}{4}\rho_{postshock} \qquad \text{(Eqn. 5.23)}$$

E Magnetopause

We may look upon the magnetopause as the boundary between the region dominated by the geomagnetic field on one side and the region dominated by the solar wind plasma pressure on the other side. We can make an order of magnitude calculation to show where this boundary will be located under normal solar wind conditions: We have seen earlier that the quantity $(B^2/2\mu_o)$ can be considered as a magnetic pressure term.

We can therefore write the condition for the location of the magnetopause by equating the total pressure on one side to the total pressure on the other side

$$P_1 + \frac{B_1^2}{2\mu_0} = P_2 + \frac{B_2^2}{2\mu_0} \qquad \text{(Eqn. 5.24)}$$

Next we assume that $\frac{B_1^2}{2\mu_0} = P_2 = 0$ which says that there is only particles on the left side and only field pressure on the right side.

The pressure is not nkT in this case, because the energy of the solar wind is a directed energy, and the resulting pressure is:

$$P_1 = nmv^2 \qquad \text{(Eqn. 5.25)}$$

where:

n = particle density
m = particle mass
v = incident particle speed

Thus

$$nmv^2 = \frac{B_2^2}{2\mu_o} \qquad \text{(Eqn. 5.26)}$$

We can also show that the compressed value of B, that is B_2 , is equal to twice the uncompressed dipole B value.

$$B_2 = 2\frac{B_{os}}{\left(r/R_\oplus\right)_s^3} \qquad \text{(Eqn. 5.27)}$$

$where\left(\frac{r}{R_\oplus}\right)_s$ = standoff distance in earth radii

$$4\frac{B_{os}^2}{\left(r/R_\oplus\right)_s^6} = 2\mu_o\, nmv^2$$

where B_0 = Equatorial surface field strength. Solving for r gives:

$$\left(\frac{r}{R_\oplus}\right)_s^6 = \left(\frac{4\,B_o^2}{2\mu_o\, nmv^2}\right)$$

can be written as

$$\left(\frac{r}{R_\oplus}\right)_s = \left(\frac{4\,B_{os}^2}{2\mu_o nmv^2}\right)^{1/6} = \text{stand off distance} \quad \text{(Eqn. 5.28)}$$

Plug in some reasonable values:

$$B_{os} = 3.0 \times 10^{-5}\ T,\ n = 10^7\ m^{-3},\ m = 1.67 \times 10^{-27}\ kg,\ v = 4 \times 10^5\ m/s$$

$$\left(\frac{r}{R_\oplus}\right)_s = \left(\frac{4\times\left(3\times10^{-5}\right)^2}{\left(10^7\right)\left(1.67\times10^{-27}\right)\left(4\times10^5\right)^2\left(8\pi\times10^{-7}\right)}\right)^{1/6} = 9.01$$

Thus under these typical conditions the standoff distance is about 9 earth radii, a value which is in tolerably good agreement with observations.

An interesting feature of this result is the fact that as a result of the (1/6) exponent even rather large changes in the solar wind will not affect the standoff distance a great deal. A change of a factor of 10 in the product nmv^2 will only change $\left(r/R_\oplus\right)_s$ by about a factor of 1.5 and that is a pretty extreme case. Thus the magnetopause is a surprisingly static boundary.

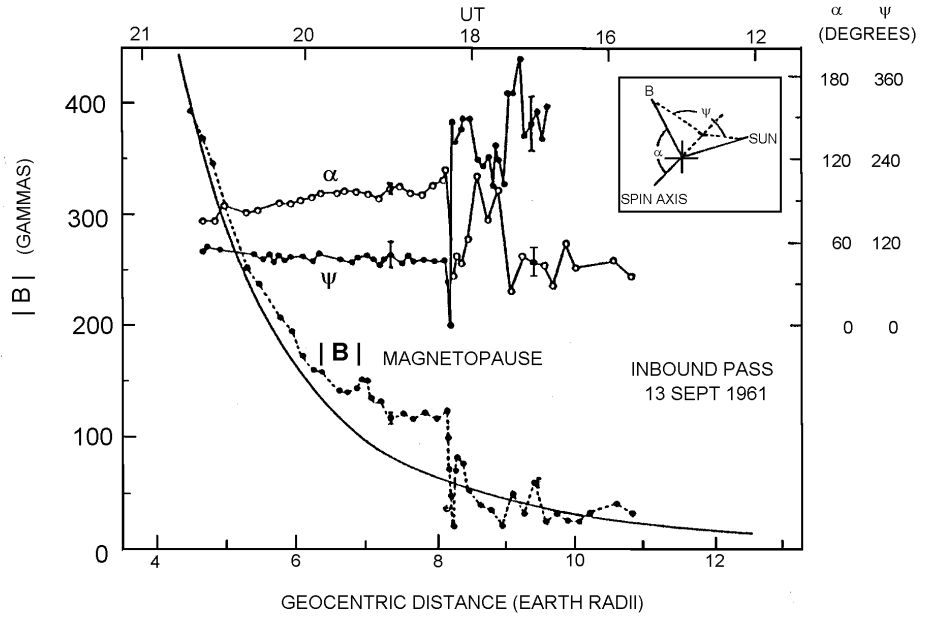

Figure 5.11 A magnetometer record of the geomagnetic field obtained near the noon meridian during an inbound pass of Explorer 12 on September 13, 1961. The magnitude of the total magnetic intensity |B| and the angles α and ψ, defined in the inset figure, are plotted against geocentric distance from the earth (1 gamma = 10^{-5} Gauss = 1 nT). The smooth curve shows the variation of |B| with distance for the *Finch and Leaton* [1957] geomagnetic reference field.

From: Cahill and Amazeen, The boundary of the geomagnetic field, in
Journal of Geophysical Research, 68, 1835-1843, 1963, or in
Planetary and Space Science, 15, 997-1033, 1967.

Found in review article: Structure of the Magnetopause, D. M. Willis, Reviews of Geophysics and Space Physics, 9, 953, 1971.

F Geosynchronous Orbit - The Plasmasphere and the Plasma Sheet

Within the magnetosphere are two regions of primary interest (as far as satellites in geosynchronous orbit are concerned). They are the plasma sheet and plasmasphere. Satellites in geosynchronous orbit will generally be in one of these two regions, depending upon the local time and the level of magnetic activity. The relative locations of these regions are partially indicated in figures 4.1 and 5.1, and are shown in cross-section views in figure 5.12. Note that the Navstar (GPS) satellites, in their 4 R_E, circular, inclined orbits, will pass through these same plasma regions.

The plasmasphere is generally thought of as the upward extension of the ionosphere, a region of relatively cold, dense plasma. The outer boundary of the plasmasphere is the plasmapause, typically found from 4-6 earth radii out, as observed at the equator. Outside this boundary region we find the plasma sheet, a region of relatively hot, tenuous plasma. Geosynchronous satellites are typically in the plasmasphere from ~ mid-afternoon (1500 Local time) to early evening (~2000 LT), and in the plasma sheet from early evening to just past dawn (~0600 LT). The region from dawn to mid-afternoon is an ambiguous region of mixed plasmas.

The region between the plasmasphere proper and the plasma sheet, as observed on the night side of the earth, is nominally the plasmapause region, which of necessity has a finite thickness. The gap between these two regions, as given by Vasyliunas, is partly an artifact of the instrumentation available at that time, but still accurately reflects the somewhat ambiguous nature of the mixed regions of hot and cold plasma just outside the plasmasphere.

The plasmasphere has as its low altitude boundary the ionosphere, a boundary which is nominally at an altitude of 1000 km, though the distinction is not a clear one. The plasma sheet begins at 5-6 earth radii at the equator, but note that the hot plasma follows the magnetic field lines up to a high latitude intercept with the ionosphere, at magnetic latitudes from 60-70°.

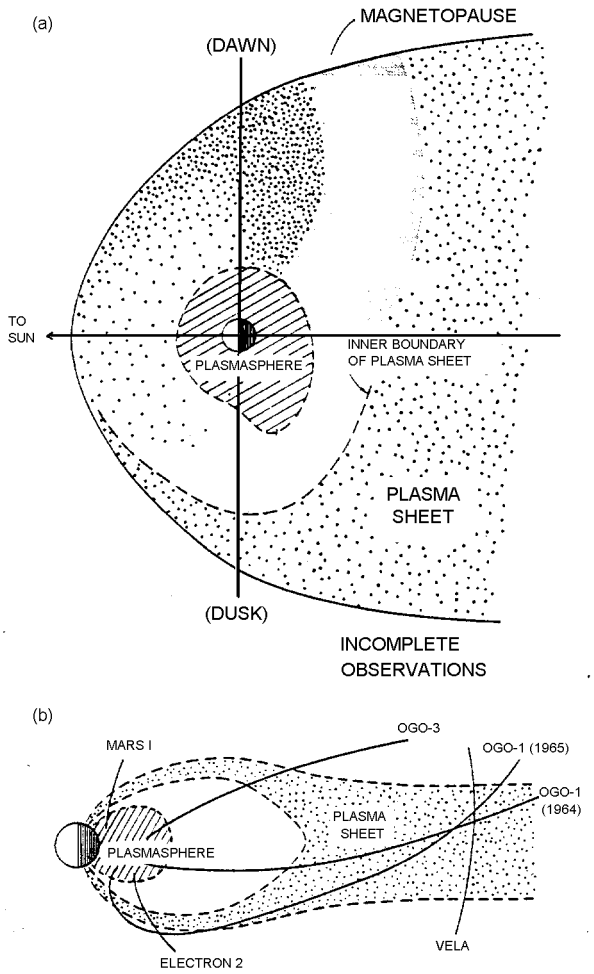

Figure 12. Diagram of the plasmasphere and plasmasheet. Illustration shows the average distribution of low-energy electrons (a) in the equatorial plane, and (b) in the meridian plane (noon-midnight slice) of the magnetosphere. Orbits of significant early satellites are indicated. Here, low energy electrons means a few hundred eV. Figure from Vasyliunas, V. M. (1972).

Vasyliunas, V. M., Magnetospheric Plasma, in *Solar Terrestrial Physics 1970*, E. R. Dyer and J. G. Roederer, eds., D. Reidel Publishing Co., Dordrecht, Holland, 1972. A survey of low-energy plasma measurements in space.

There is a high latitude limit, corresponding to magnetic field lines extending out 10's to 100's of earth radii, depending upon magnetic activity.

As noted above, the plasmasphere is a region of cold, 'dense' plasma near the earth, extending out to geosynchronous orbit at times. The density of the plasma inside the plasmasphere ranges from

a peak value of ~10^4/cm^3 down to ~1 cm^{-3}. Data from OGO-5 show a variety of plasma (ion) density profiles obtained in 1968 (Figure 5.13). It can be seen that there is a gradual slope at low "L", followed by a sharp drop in density. The gradual slope is a reflection of the increasing volume of the magnetic field 'flux' tubes, and it is often found that the total plasma density is inversely proportional to the fourth power of L.

$$n\ (\ cm^{-3}\ ) = 100\ \left(L/4.5\right)^{-4} \qquad \text{(Eqn. 5.29)}$$

The plasmasphere ions and electrons are 'cold' with characteristic temperatures of 0.5 - 1.0 eV. There are equal numbers of ions and electrons (the quasi-neutrality condition), and the ions are primarily H+ and He+, with a smaller percentage (usually) of O^+, O^{++}, N^+, He^{++}, and N^{++}.

The plasmasphere is said to 'co-rotate' with the earth. The cold plasma is well tied to the earth's magnetic field. Corresponding to this motion is an electric field, just sufficient to produce the observed E x B 'drift'. At any rate, this effect drops off outside the plasmasphere, more or less near geosynchronous orbit.

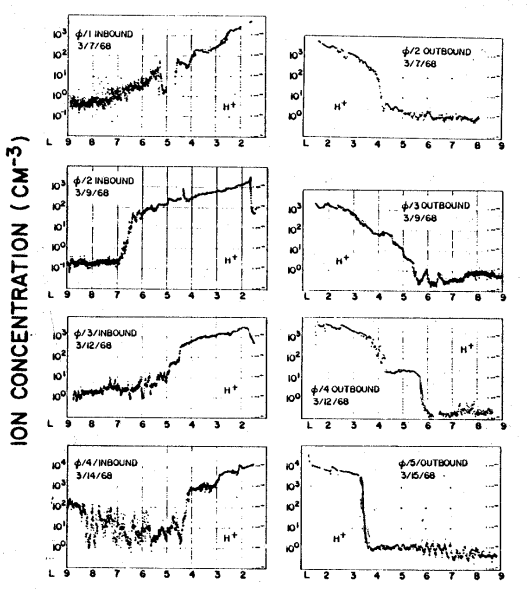

Figure 5.13 H^+ density distribution ($n_i(L)$) profiles from ion mass spectrometer data obtained on board the OGO-5 satellite. Here, L measures the equatorial distance in earth radii R_E = 6375 km (from Harris et al, 1970)

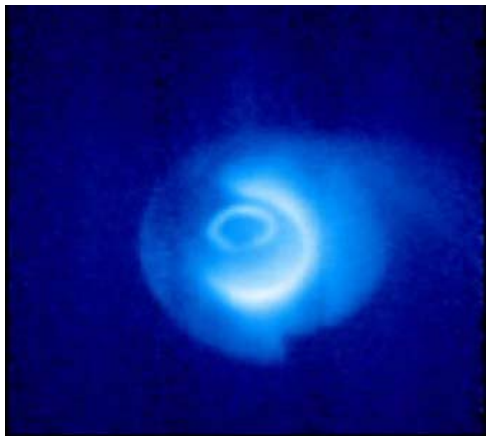

Figure 5.14 Image satellite observations of He+ (HE II) at 304 Å. (Not unlike viewing the sun from SOHO – just not nearly as bright !) IMAGE was launched March 25, 2000. Image from May 2000 ? Satellite near apogee – 6-7 R_E.

The plasma sheet is the region of hot plasma (T~>1 keV) with a typical density of ~1/cm^3. During magnetic 'substorms' the temperature of the plasma sheet electrons can reach 10-20 keV, and substantial fluxes of electrons are seen at energies up to 50-100 keV. The ions which make up the plasma sheet generally show about a 50-50 mixture of singly charged hydrogen (H^+) and oxygen (0^+). These ions are thought to come from the upper atmosphere of the earth (because we see 0^+, a terrestrial ion, as opposed to He^{++} or O^{6+}, solar wind ions).

The plasma sheet is typically thought of as being a feature of the night-side of the magnetosphere, particularly the midnight-to-dawn sector, though the hot plasma can drift around the earth into the dawn-noon sector. It extends from L~5 or 6 to beyond L=20. the location of the inner boundary depends on magnetic activity. During a period of high activity (high Kp, and many substorms), the plasma sheet may extend in to L = 3 or 4, and will be seen at geosynchronous orbit from near dusk, through midnight, and on past dawn.

Modern data from a particle detector on an operational geosynchronous satellite are shown in figure 5-15. The satellite is in the plasmasphere from 0-4 UT, then moves into the plasma sheet for the rest of the day. Local midnight occurs at 1100 UT. This is roughly where the hottest (most energetic) electrons are seen. Note that this is a fairly quiet period, but the electrons observed at local midnight extend to many keV.

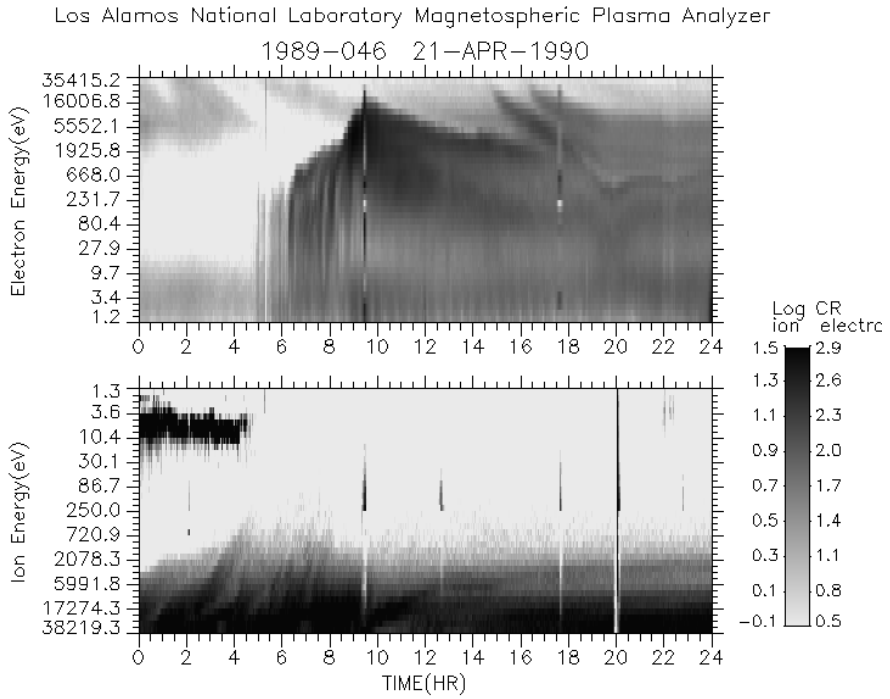

Figure 5-15 Ion and electron observations from the LANL charged particle analyzers on the geosynchronous satellite, 1989-046. Data are plotted such that low energy electrons are at the lower boundary of the top panel, while the ion data are inverted, with lowest energies at the top. This facilitates the comparison of the lower energy electron and ion data. High fluxes of low energy ions (3-10 eV) are seen from 0-4 UT, indicating that the satellite is in the plasmasphere. Relatively high fluxes of more energetic electrons begin to appear at 0600 UT, roughly dusk local time.

G Magnetospheric Convection

Why do the data at geosynchronous orbit appear as they do? A reasonable explanation for the patterns observed was obtained in the first decade of space plasma physics, and the theory has remained reasonably consistent since that time. The answer lies in magnetospheric convection and drifts. The concept was nominally due to Neil Brice, at NASA/GSFC, and has been termed Brice convection. Atsushiro Nishida developed the concept in an early classic text on the topic.

A) Because of the flow of the solar wind past the magnetosphere, and the processes being driven at the magnetopause, there is imposed on the magnetosphere an electric field in the dawn-dusk direction with a magnitude of ~ 1 mV/m. This electric field is such as to force plasma sunward from the tail, a region where we believe hot plasmas are created. Note that integrated over the magnetosphere, there is a 50-80 kV potential drop associated with this electric field.

B) Because the inner magnetospheric region called the plasmasphere is corotating with the earth, there must be a radial electric field (inward) associated with the plasma rotation. For zero energy particles, the balance between these two competing fields determines a set of boundaries, most easily determined by calculating the equipotential surfaces.

Following Parks (1991), we obtain the corotation field in the equatorial plane:
In spherical coordinates:

$$\vec{\mathbf{U}} = \omega\, r\, \hat{\boldsymbol{\phi}} \qquad \text{(Eqn. 5.30)}$$

$$\mathbf{B} = B_o \left(\frac{R_\oplus}{r} \right)^3 \left(-\hat{\boldsymbol{\theta}} \right) \qquad \text{(Eqn. 5.31)}$$

where U is the streaming, or drift velocity. The frozen-in-field condition gives:

$$\mathbf{E}_{corotation} = -\mathbf{U} \times \mathbf{B} = \omega\, r\, \hat{\boldsymbol{\phi}} \times B_o \left(\frac{R_\oplus}{r} \right)^3 \left(\hat{\boldsymbol{\theta}} \right) = \frac{\omega\, B_o R^3}{r^2} \left(-\hat{\mathbf{r}} \right) \qquad \text{(Eqn. 5.32)}$$

The corresponding potential is easily shown to be:

$$\Psi_{corotation} = -\frac{\omega B_o R_\oplus^3}{r} = -\frac{\omega B_o R_\oplus^2}{L} \qquad \text{(Eqn. 5.33)}$$

The cross-tail electric field can be expressed as:

$$\mathbf{E}_{sw} = E_{sw}\, \hat{\mathbf{y}}, \quad \text{where } \hat{\mathbf{x}} \text{ is sunward, } \hat{\mathbf{z}} \text{ is north, and hence } \hat{\mathbf{y}} \text{ is from dawn to dusk} \qquad \text{(Eqn. 5.34)}$$

$$\Psi_{sw} = -E_{sw} y = -E_{sw} r \sin\phi = -E_{sw}\, L\, R_\oplus \sin\phi \qquad \text{(Eqn. 5.35)}$$

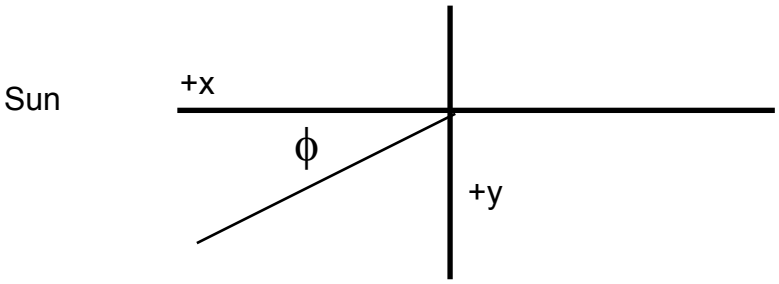

Adding the two potentials together, we obtain

$$\Psi_{total} = -E_{sw}\, L\, R_{\oplus} \sin\phi - \frac{\omega\, B_o R_{\oplus}^2}{L}$$

The resulting equipotential contours are illustrated in Figure 5.16. It can be seen that there are two distinct regions. In the region near earth, the equipotential lines are closed, and ~circular. These are streamlines for the drift of ~zero energy particles (no significant ∇B drift). Outside the curiously pointed boundary crossing the duskward axis at L=7.5, the streamlines are 'open', meaning the plasma flowing along these lines from the tail will pass by the earth, terminating at the magnetopause.

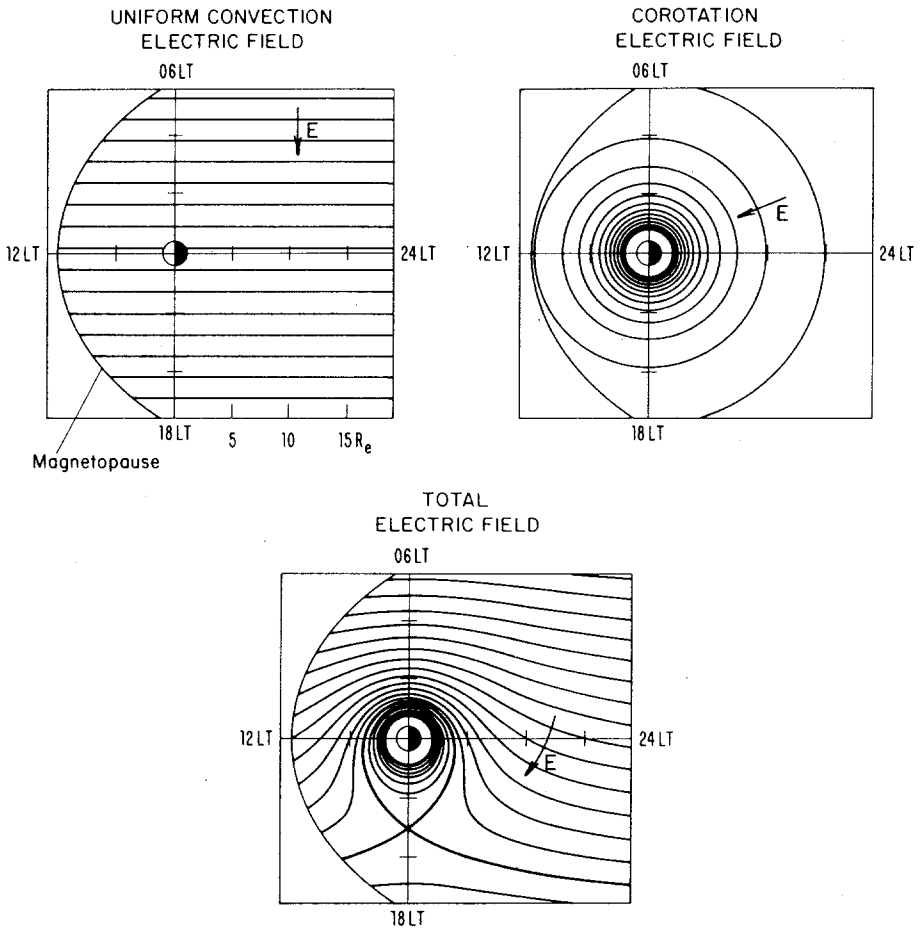

Figure 5.16 Lyons, L.R., and D. J. Williams, *Quantitative Aspects of Magnetospheric Physics*, D. Reidel Publishing Co. Boston, MA, 1984
Found in: George K. Parks, *Physics of Space Plasmas,* Addison-Wesley Publishing Co., Redwood City, CA, 1991, page 234.

A formula for the location of this boundary can be obtained by recognizing that it is the boundary between the region where the solar wind induced, cross-tail field dominates, and the region where corotation dominates. Dealing just with the magnitudes at 1800 LT:

$$E_{corotation} = \frac{\omega\, B_o\, R_\oplus}{L^2} = E_{SW},\ \text{or}\ L_{Plasmapause} = \sqrt{\frac{\omega\, B_o\, R_\oplus}{E_{SW}}} \qquad \text{(Eqn. 5.36)}$$

$$L_{plasmapause}(1800) = \sqrt{\frac{\omega\, B_o R_\oplus}{E_{sw}}} = \sqrt{\frac{2\pi}{86400}\frac{3\times10^{-5}\bullet 6.37\times10^{6}}{0.35\times10^{-3}}} = 6.3 \qquad \text{(Eqn. 5.37)}$$

If particles with significant kinetic energy are considered, then the grad-B drift must be included, at least near the earth. The grad-B drift is azimuthal, and for electrons, is in the same direction as co-rotation. This term has the effect of expanding the corotation equipotentials - and the seperatrix moves outward.

For ions, the grad-B drift opposes the corotation field, and for sufficiently high energies (above ~ 5 keV at geosynchronous orbit), they will counter-rotate. In close to the earth, it is the grad-B drift of the ions which produces the ring-current.

H The Radiation Belts

1 The Van Allen Radiation Belts

The (Van Allen) radiation belts, are of primary concern for the satellite designer because of the effects of penetrating radiation on electronics. The Van Allen belts permeate the plasmasphere and inner plasma sheet, but are generally thought of as co-existing with the plasmasphere. It is the particles of the radiation belts that primarily form the ring current.

Figure 5.17 shows the ion flux vs. L, with ion energy as a parameter. For purposes of study, focus on two energies which illustrate the main points here. Ions of 1 MeV energy have a peak flux at L ~ 3. This would be the nominal location of the canonical 'ring current'. The L value at which the peak flux occurs decreases as energy increases. The 400 MeV ions, for example, have a peak flux at L ~ 1.5. (These plots are based on the standard NASA model held at the National Space Science Data Center, and is commonly attributed to Jim Vette.)
(http://nssdc.gsfc.nasa.gov/space/model/magnetos/aeap.html)

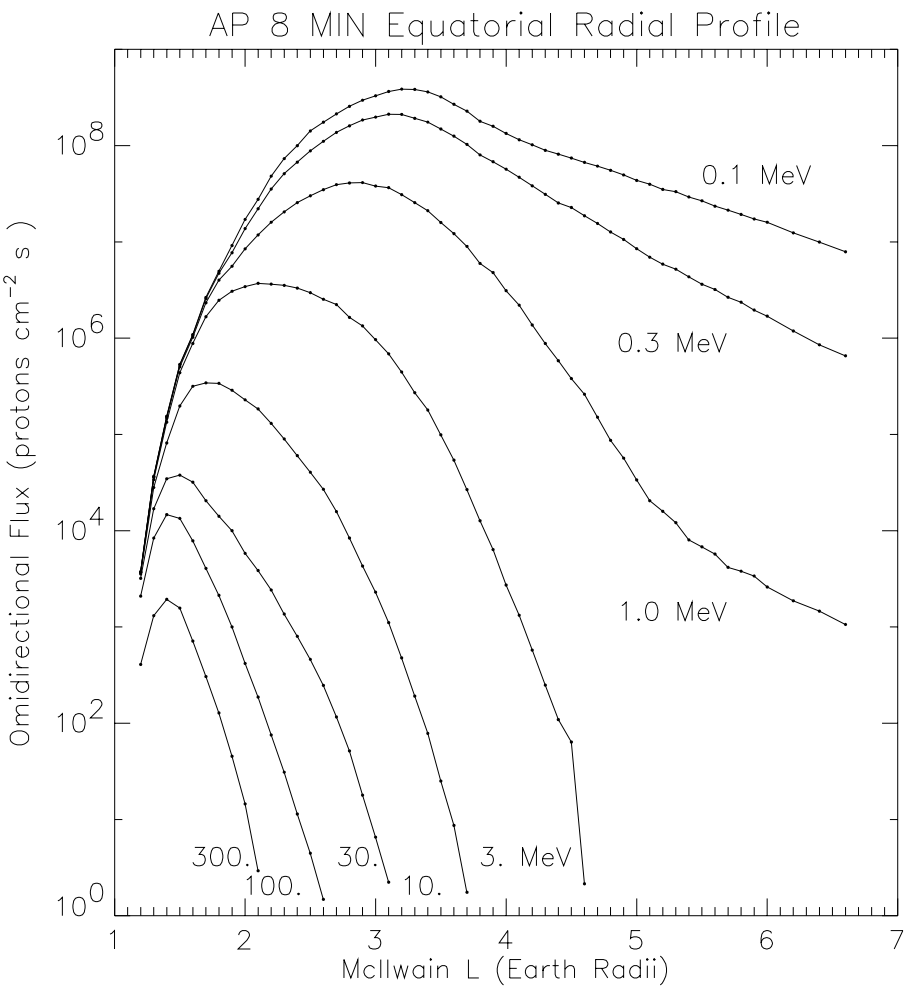

Figure 5.17 Radiation belt ion flux vs. L. The plotted values are from the AP8MIN model for omnidirectional flux of protons (ions) in the equatorial plane with energies above threshold values between 0.1 and 400.0 MeV [Sawyer and Vette, 1976][http://nssdc.gsfc.nasa.gov/space/models/trap.html].

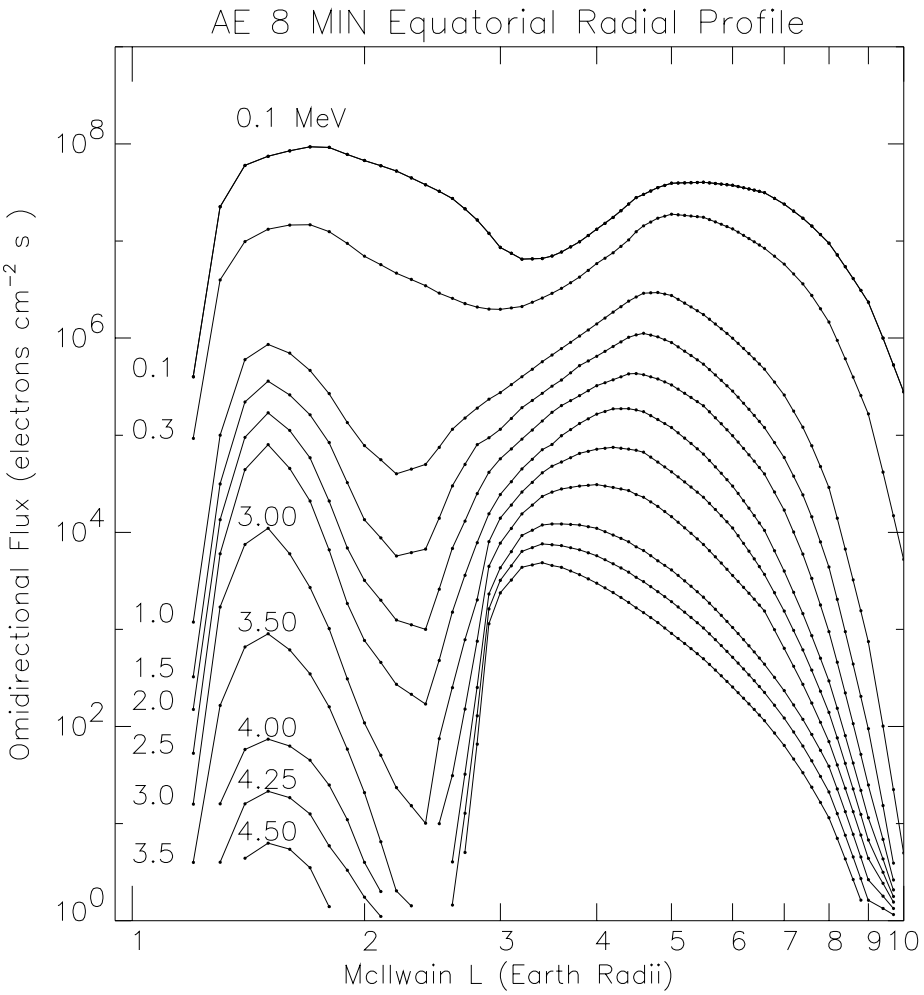

Figure 5.18 Radiation Belt Electrons - Solar Minimum. The curves are labeled with the electron energy in MeV, ranging from 0.1 to 4.5 MeV. Note the logarithmic horizontal axis. Graphed data obtained from the National Space Science Data Center, at NASA/GSFC. http://nssdc.gsfc.nasa.gov/space/models/trap.html

Figure 5.18 shows the electron flux vs. L, with electron energy as a parameter. Again we focus on two energies which illustrate the main points here. Electrons of 1 MeV energy have a peak flux at L ~ 1.5, coinciding with the so-called, 'inner belt', and the location of the highest energy ions. There is a second peak at L ~ 5, coinciding with the more traditional ring current, and (relatively) lower energy ions.

Given the above characteristics for the average condition of the radiation belts, we again come to the question of why they take the form shown above, and what are the significant variations about the model values shown so far. It is now also appropriate to see how the radiation belts are related to the phenomenon observed in ground magnetometer data, in particular, the ring current.

2 The Ring Current

Since the ring current was originally described to you as an inference from the magnetic storm data (e.g. Dst and discussion), we return briefly to that point of view. First of all, does the observed distribution of energetic particles explain the variation in magnetic field strength ascribed to a 'ring current' ? The answer is yes.

The magnetic field perturbation produced by the particles extends into space, and suitably clever manipulation of the observations allows one to show that the observed particles are capable of producing the observed perturbation in magnetic field. Note that the current is primarily produced by grad-B drift of protons.

What are these ring current ions, and where do they come from ? Many of the plots you see, are generally labeled 'protons', but are really for all ions. This is because most of the early instruments, and many of the current ones, such as NOAA-10 detectors, do not discriminate between ions. It is desirable to do so, however, so that one can sort out where these ions come from, and then understand the formation and decay of the ring current.

If we look again at a typical magnetic storm signature (Dst), we find two main puzzles. Where do the particles come from, and where do they go. First, let's concentrate on the decay of the ring current, also termed the storm recovery phase. We start there, because it's better understood.

Two concepts come up, at this point, which have been presented above:

a) there are low energy charged particles for the ring current to interact with, e. g. the plasmasphere, and

b) there is a neutral gas background to interact with, as revealed by the geocorona (addressed next).

The low energy charged particles of the plasmasphere (described above) can interact with the ring current via the medium of electromagnetic waves (photons). A particularly important subset of such waves are the waves (radio signals) at a few kilo-Hertz frequency, known as whistlers. These waves are generated, initially, by lightning in the atmosphere. The waves travel into space, where they can scatter off the charged particles (photon collides with particle, transfers momentum, changes pitch angle). If the particle is knocked into the loss cone, it will fall into the atmosphere, and be lost. This works particularly well for the high energy electrons. It is less important for ions. Note that because there are lots of low-energy electrons and ions in the plasmasphere; it doesn't affect charge neutrality if a few of the MeV particles are knocked out.

Ions are traditionally thought of as being lost via charge-exchange with the neutral hydrogen background. This background is revealed in the observations of neutral hydrogen made in the UV (Lyman-alpha) of the near-earth region.

3 The geocorona

The uppermost region of the neutral atmosphere is a region of neutral hydrogen gas extending well into near-earth space. This gas is visible in reflected UV sunlight in the Lyman-α emission (scattering). This light is termed the geocorona. Figure 5.19a shows the geocorona, as observed from the Moon by Apollo astronauts (taken with an NRL camera). This light is a visible indication of the neutral hydrogen background which is effectively the top of the earth's atmosphere. The glow can be modeled, and from that the neutral hydrogen density profile can be determined. Figure 5.19b shows a model developed by Rairden, using data from the DE-1 satellite. The neutral hydrogen density at geosynchronous orbit is about 10 / cm^3 - about the same as the plasma density, depending upon local time.

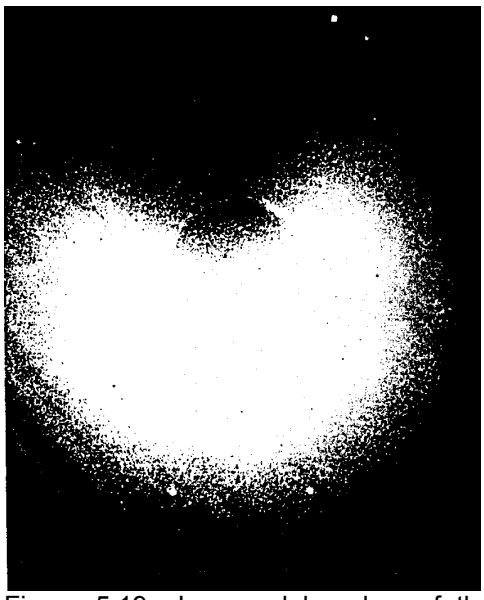

Figure 5.19a Lyman-alpha glow of the geocorona photographed from the moon. The earth-centered cloud reaches 50,000 miles, and its intensity exceeds the total of all visible airglow.

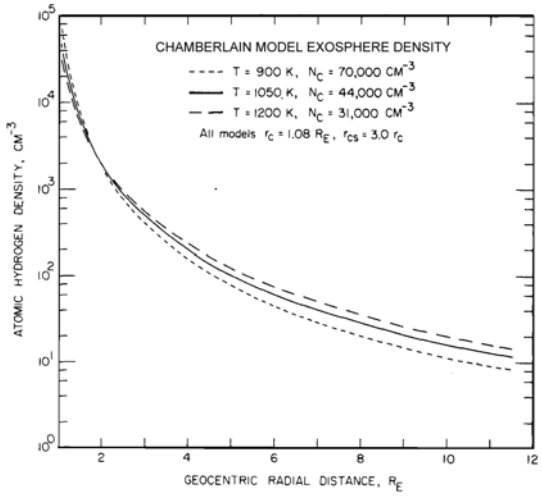

Figure 5.19 b. Exospheric hydrogen density versus radial distance for the Chamberlain model. The model at temperature T = 1050 K provides the best fit to the DE 1 geocoronal observations.

From: Geocoronal imaging with Dynamics Explorer, R. L. Rairden, L. A. Frank, and J. D. Craven, Journal of Geophysical Research, vol. 91, page 13613, 1986.

4 Ring Current Decay and Composition

This neutral gas background provides a scattering mechanism for the energetic ions of the radiation belts. This process is illustrated in Figure 5.20. An energetic ion will collide with a low energy neutral particle, and take the electron away. There is now an energetic neutral atom, which heads off towards Pluto, and one more (boring) low energy (~0.1 eV) proton. This is a well understood physical process, and the time scale for decay via charge exchange was one of the first quantitative calculations to be done.

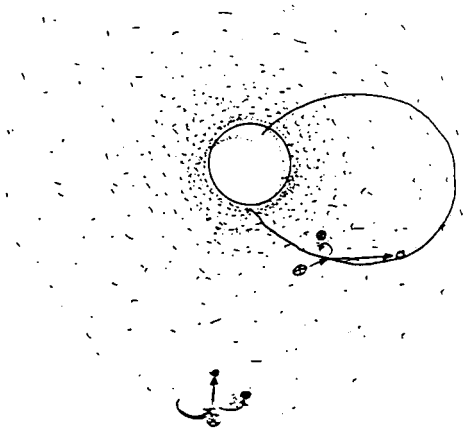

Figure 5.20 During charge exchange a **hot** (or energetic) ion collides with a **cold** neutral hydrogen atom, the same neutral hydrogen "visible" in the UV as the geocorona. The **hot** ion picks up an electron from the **cold** H atom and becomes a **hot** neutral particle, which is no longer trapped in the earth's magnetic field. The **cold** H, which lost its electron, is now trapped instead. Thus the process causes a loss of the energetic ions from the ring current. [This figure provided by Joe Fennell.]

These charge exchange calculations, which assumed that the ring current was composed only of protons, were inconsistent with some observations, however, of the type shown in figure 5.20. The time scales for decay of ring current ions indicated that there must be more than one kind of ion out there, and that the initial rapid recovery of the ring current is inconsistent with H+ being the (initial) primary component of the ring current. We now understand that the ring current, as formed during magnetic storms, is composed of O+, He+, and H+. The heavier ions decay more quickly, as indicated by figure 5.21, indicating that there was indeed substantial amounts of oxygen (and helium) in the ring current. This helps address the question of where the ring current particles originate.

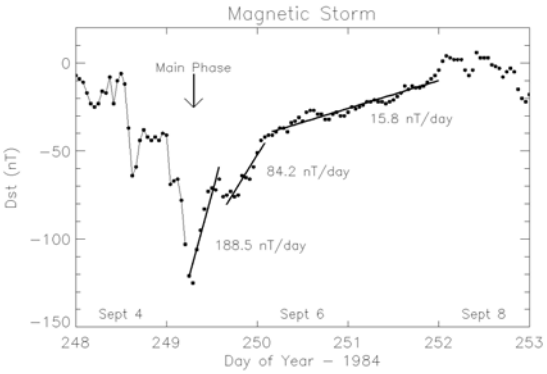

Figure 5.21 The recovery phase of the magnetic storm exhibits several characteristic time scales, corresponding to the different elements (ions) which make up the ring current. These time scales are revealed by the 3 characteristic slopes found during the storm illustrated here. In sequence, they reveal the decay of the O^+, He^+, and finally H^+. The 3 time scales are due to the different cross-sections for the collision process of charge-exchange.

Where does the ring current come from ? What is it made of ? Where does it get all that energy ?

Initially, people thought the ring current ions must come from the sun, since the earth could not (apparently) accelerate ions and electrons to the observed energies. Observations of the mass composition of the ring current show this to be incorrect. Figure 5-21 shows the relative abundance of several oxygen ions in the ring current during the storm illustrated in Figure 5-20. This is the first direct measurement of ring current composition. Oxygen was found to be the major ring current component of the initial phase of the storm, in singly charged form. Where does it come from ? The ratio of 0^+ (and 0^{++}) to 0^{6+} (oxygen stripped of 6 electrons) show that ions which originate in the earth's atmosphere dominate those of solar origin. The ring current ions must come from the earth's atmosphere.

How are they energized ? We don't know. If you look in the magnetosphere for a power source, there is the cross-tail electric field, which is good for 100 keV or so. The major alternative is the dB/dt of a storm which should induce a good size voltage around the earth.

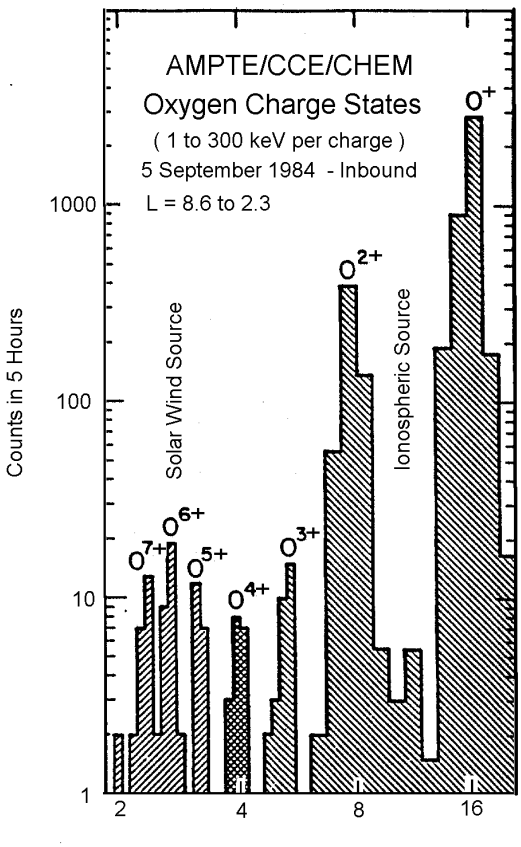

Figure 5.22 Charge-state histogram of 1 to 300 keV/e ring current oxygen during the Sept 4-7, 1984 geomagnetic storm. Measurements were made on the AMPTE/Charge Composition Explorer (AMPTE/CCE) satellite, with the CHEM experiment, built by the University of Maryland and the Max Planck Institut. Notice the *extremely* long accumulation interval.

From: First composition measurements of the bulk of the storm-time ring current (1 to 300 keV/e) with AMPTE-CCE, G. Gloeckler, B. Wilken, W. Stüdemann, F. M. Ipavich, D. Hovestadt, D. C. Hamilton, and G. Kremser, Geophysical Research Letters, vol. 12, page 325, 1985.

Figure 5.23
Recently, the radiation belts have been observed by the IMAGE satellite, using the charge-exchanged ions escaping from the magnetosphere. The satellite is viewing from the sun towards the Earth, viewing the cloud beyond the Earth on the night side.

This image is a convolution of the intensity of the radiation belts, and the dcnsity of the neutral hydrogen background.

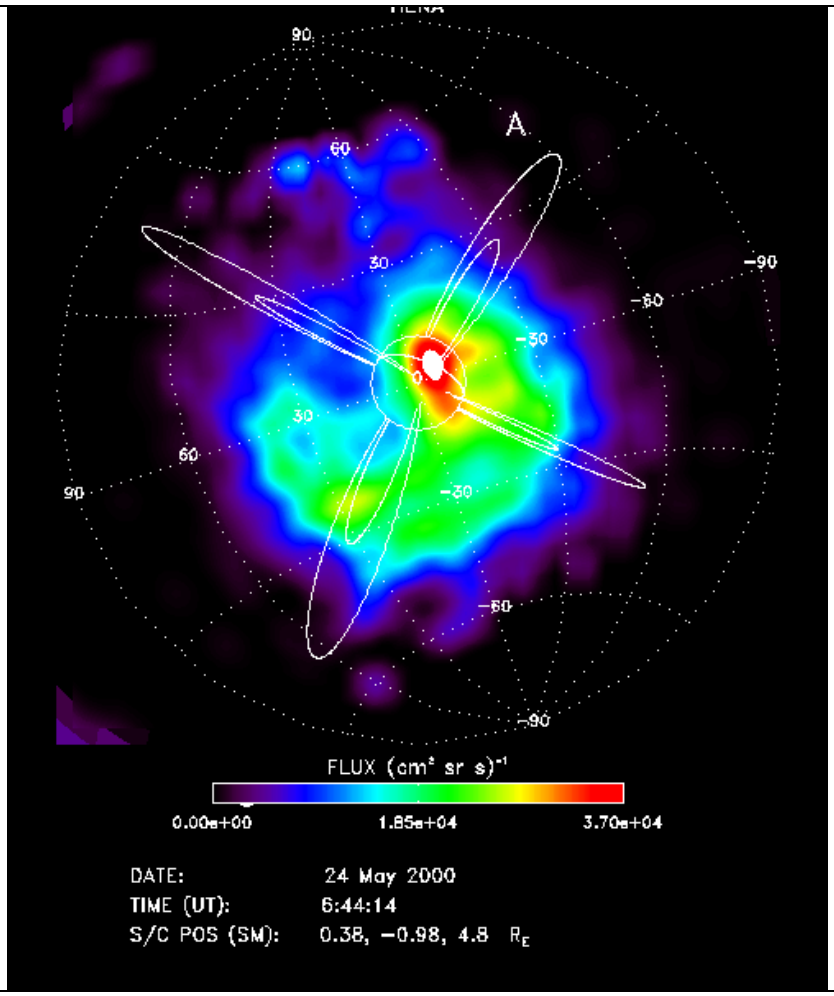

I Problems

1. Calculate the magnetopause standoff distance for shock conditions - v~ 800 km/s, n = 25 cm^{-3}.

2. The electric field in the plasmasphere is just such as to cause the cold plasma to 'corotate' with the earth. What is the electric field necessary to proud this effect ? (magnitude and direction) The answer is given in section 5.8.
Calculate and plot E(r) from L = 1 to 6.
($B_o = 3 \times 10^{-5}$ Tesla, $R_\oplus = 6.7 \times 10^6$ m)

3. Calculate the Invariant latitudes which correspond to L =4, and L = 6.6.

4. Compare the L^{-4} electron density profile (Eqn. 5.29) with the Rairden article profile for neutral hydrogen density (Figure 18b). Do this by making a plot, and evaluating the two quantities at ~1 $R_\oplus$ intervals. Is there a point where there are more electrons (and presumably ions) than there are neutral H atoms ?

5. For 1 MeV ions, at L = 3, calculate the grad - B drift velocity.
Assume a dipole magnetic field.
Assume the pitch angle (α) is 90°.

Note: $\nabla |\vec{B}| = \frac{\partial}{\partial r}\left\{ B_o \left(\frac{R_\oplus}{r}\right)^3 \right\} = -3\left(\frac{|\vec{B}|}{r}\right)\hat{\mathbf{r}}$ in the magnetic equatorial plane,

hence $\frac{\nabla |\vec{B}|}{|\vec{B}|} = -3\,\hat{\mathbf{r}}/r$

6. Estimate the density for 1 MeV protons at L = 3. Use the model found in Figure 5-16, which shows the flux ~ 3×10^7 (ions/cm^2 s). It might help to know that the flux, f = nv, where v is the average velocity. The average velocity can be found by solving the well known equation $K = \frac{1}{2} mv^2$, after carefully converting the energy from MeV to Joules, and the flux from ions/cm^2 s to ions/m^2 s. You pretty much have to assume the ions are protons (m = 1.67×10^{-27} kg)

7. Estimate the current density (J = qnv) due to 1 MeV protons, where the velocity is the grad-B drift velocity. By assuming this current density flows through a box 1 earth radius on a side, one can estimate a total current, I = J* Area. Estimate I, and compare it to the current calculated in chapter 4 homework as being required to produce the observed Dst..

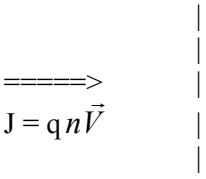

8. Use Faraday's law to calculate the electric field induced around the earth during a storm, ignoring the fact that much of this dB / dt is produced by the particles, themselves.

dB ~ 100 nT, dT = 100 -1000 s, r = 3 Re (20,000 km)

9. Evaluate the magnetic field strength for L = 5, λ_m = 0°, 45°, then calculate the critical (equatorial) pitch angle such that particles which will mirror at λ_m = 45°.

10. Magnetospheric Convection: The plasmapause potential contour illustrated in Figure 5.15 can be obtained by returning to the convection discussion, and solving for the first closed contour.

a) Using, $L_{plasmapause}\left(\phi = 90^{\circ}\right) = \sqrt{\dfrac{\omega B_o R_{\oplus}}{E_{sw}}}$ (at 1800 LT),

solve for $\Psi_{plasmapause}$ (at ϕ=90° or 1800 LT). (A formula which is a function of E_{sw})(Use Eqn. 5.33)

b) Solve the equation: $\Psi_t = -E_{sw} L R_{\oplus} \sin\phi - \dfrac{\omega B_o R_{\oplus}^2}{L}$ for L and show that the following relation can be obtained:

$$L = \frac{\Psi_t}{A} \pm \left[\left(\frac{\Psi_t}{A} \right)^2 - \frac{2\omega B_o R_{\oplus}^2}{A} \right]^{\frac{1}{2}} \quad ; \quad \text{where } A = 2 E_{sw} R_{\oplus} \sin\phi$$

c) Now solve for an equation that gives $L_{plasmapause}$ as a function of φ. You do this by plugging in the potential you got in part (a) into the equation you obtain in part (b).

d) Now plot $L_{plasmapause} = L(\phi)$, with E_{sw} as a separate parameter. (E_{sw} =0.1, 0.3, and 1.0 mV/m). A polar plot is the best way to present the results. Which produce the result in most obvious agreement with expected locations for the plasmapause?

11. Calculate the energies for which the corotation electric field induced drift velocity $\vec{\mathbf{U}} = \omega r \hat{\boldsymbol{\phi}}$, equals the ∇B drift velocity, for protons at L = 3, and L = 6.6. For simplicity, work in the equatorial plane, and look only at the grad-B drift.

Note:

$$\vec{v}_D = \frac{K_\perp}{qB} \frac{\vec{\mathbf{B}} \times \nabla B}{B^2} \quad ; \quad \nabla B = -\frac{3}{r} B \hat{\mathbf{r}} \ (\lambda = 0); \quad \left. \frac{\vec{\mathbf{B}} \times \nabla B}{B^2} \right|_{\lambda=0} = -\frac{3}{r} \left(-\hat{\boldsymbol{\theta}} \right) \times \hat{\mathbf{r}} = -\frac{3}{r} \hat{\boldsymbol{\phi}}$$

$$\vec{v}_D = -\frac{3}{r} \frac{K_\perp}{qB} \hat{\boldsymbol{\phi}}$$

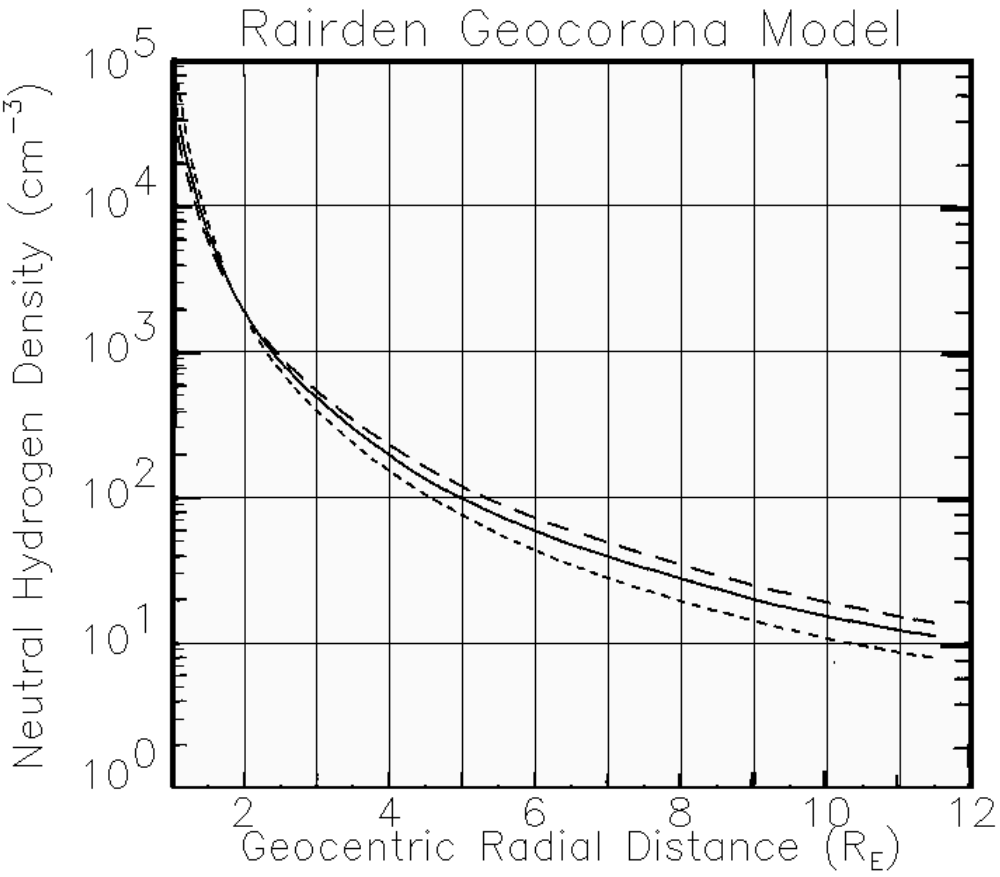

Homework Problem 5.4